HHS Public Access

Author manuscript

J Biomed Mater Res A. Author manuscript; available in PMC 2017 August 01.

Published in final edited form as:

J Biomed Mater Res A. 2016 August ; 104(8): 2037–2048. doi:10.1002/jbm.a.35738.

Intracellular calcium and cyclic nucleotide levels modulate neurite guidance by microtopographical substrate features

Shufeng Li[1,3], **Bradley Tuft**[2,‡], **Linjing Xu**[1], **Marc Polacco**[1,§], **Joseph C. Clarke**[1,#], **C. Allan Guymon**[2], and **Marlan R. Hansen**[1,4,*]

[1]Department of Otolaryngology-Head and Neck Surgery, University of Iowa, Iowa City, IA 52242, USA

[2]Department of Chemical, University of Iowa, Iowa City, IA 52242, USA

[3]Department of Otolaryngology, EYE & ENT Hospital of Fudan University, Shanghai 200031, China

[4]Department of Biochemical Engineering and Neurosurgery, University of Iowa, Iowa City, IA 52242, USA

Abstract

Objective—Micro- and nano-scale surface features have emerged as potential tools to direct neurite growth into close proximity with next generation neural prosthesis electrodes. However, the signaling events underlying the ability of growth cones to respond to topographical features remain largely unknown. Accordingly, this study probes the influence of $[Ca^{2+}]_i$ and cyclic nucleotide levels on the ability of neurites from spiral ganglion neurons (SGNs) to precisely track topographical micropatterns.

Approach—Photopolymerization and photomasking were used to generate micropatterned methacrylate polymer substrates. Dissociated SGN cultures were plated on the micropatterned surfaces. Calcium influx and release from internal stores were manipulated by elevating extracellular K^+, maintenance in calcium-free media, or bath application of various calcium channel blockers. Cyclic nucleotide activity was increased by application of cpt-cAMP or 8-Br-cGMP.

Main results—Elevation of $[Ca^{2+}]_i$ by treatment of cultures with elevated potassium reduced neurite alignment to physical microfeatures. Maintenance of cultures in Ca^{2+}-free medium or treatment with the non-selective voltage-gated calcium channel blocker cadmium or L-type Ca^{2+} channel blocker nifedipine did not signficantly alter SGN neurite alignment. By contrast, ryanodine or xestospongin C, which block release of internal calcium stores via ryanodine-sensitive channels or inositol-1,4,5-trisphosphate receptors respectively, each significantly decreased neurite alignment. Cpt-cAMP significantly reduced neurite alignment while 8-Br-cGMP significantly enhanced neurite alignment.

*Correspondence: Marlan R. Hansen, MD Address: Dept. of Otolaryngology-HNS, Univ. of Iowa, Iowa City, IA 52242; marlan-hansen@uiowa.edu; Phone: (319) 353-7151; Fax: (319) 356-4547.

‡Dow Corning Corporation, 3901 S Saginaw Rd, Midland, MI 48640

§Section of Otolaryngology-Head and Neck Surgery, Dartmouth-Hitchcock Medical Center, Lebanon, NH 03756

#Oregon Ear Nose and Throat Center, 1170 Royal Avenue, Medford, OR 97504

Conclusion—Manipulation of $[Ca^{2+}]_i$ or cAMP levels significantly disrupts neurite guidance while elevation of cGMP levels increases neurite alignment. The results suggest intracellular signaling pathways similar to those recruited by chemotactic cues are involved in neurite guidance by topographical features.

Keywords

calcium; cyclic nucleotide; nerve guide; spiral ganglion neuron; surface topography; micropatterning; photopolymerization

1. Introduction

Precise spatial targeting of neurite growth is critical to the formation of functional neuronal circuits during neural development or regeneration. Analogously, precisely directing *de novo* neurite growth into close proximity, or even contact, with stimulating or recording electrodes will enable significant performance improvements in next generation neural prosthetics. Neurite pathfinding is accomplished as the growth cone senses and responds to a range of environmental information including biochemical and biophysical (e.g. topographical) cues. Accordingly, neural engineers have sought to create specific patterns of neural guidance cues to precisely guide neurite growth toward desired targets. For example, gradients or patterns of bioactive proteins that influence growth cone turning are used to specify the trajectory of neurite regeneration [1–3].

More recently, micro- and nano-scale surface topographical features have emerged as potential tools to control neurite growth, neural polarity and circuitry [4–13]. For example, microtopographical features generated by photopolymerization of methacrylate polymer systems direct neurite growth of spiral ganglion neurons (SGNs), trigeminal ganglion neurons, dorsal root ganglion neurons, cerebellar granular neurons, and PC-12 cells [12,14–16]. However, unlike the mechanisms underlying biochemical guidance of neurite growth that have been thoroughly investigated [17,18], our understanding of how growth cones sense topographical features and transduce those cues into directed neurite growth is limited [19,20]. Recently, microtopographical features were shown to activate TRPV1 channels and, subsequently, RhoA signaling pathways to direct neurite growth [21].

Accumulating evidence reveals the essential role of $[Ca^{2+}]_i$ in chemotropic growth cone guidance [22–25]. Whether attractive or repulsive, chemical guidance cues elicit an asymmetric $[Ca^{2+}]_i$ response in growth cones with the higher $[Ca^{2+}]_i$ concentration at the side facing the source of guiance cues. Furthermore, the baseline calcium levels alter the attractive and repulsive reponses of growth cones to guidance cues [26]. In addition to $[Ca^{2+}]_i$, cyclic nucleotides including cyclic adenosine monophosphate (cAMP) and cyclic guanosine monophosphate (cGMP) also play an important role in growth cone steering [27,2829–31].

Given the recent evidence that implicates intracellular signaling events similar to those recruited by chemorepulsive biochemical cues as a mechanism whereby topographical surface features direct neurite growth [21], we sought to determine the influence of $[Ca^{2+}]_i$ and cyclic nucleotide levels on the ability of neurites to sense and respond to simple topographical micropatterns. The spatial and temporal control of photopolymerization is

used to fabricate micropatterned methacrylate polymer substrates to probe this crucial relationship. Dissociated cultures of spiral ganglion neurons (SGNs), the target neurons of the cochlear implant which is the most widely used and successful neural prosthesis, were plated on the micropatterned substrates. We find that elevation of $[Ca^{2+}]_i$ or cAMP levels disrupts neurite alignment to physical cues while elevation of cGMP levels enhances neurite alignment.

2. Materials and methods

Photopolymerization to generate micropatterned substrates

To investigate neurite growth cone sensing of biophysical cues, photopolymerization was used to generate micropatterned surfaces with various widths and depths as described elsewhere [12,14,16]. Briefly, the monomer mixtures of 39 wt% hexyl methacrylate and 60 wt% 1,6-hexanediol dimethacrylate (Sigma-Aldrich, St. Loius, MO) with 1 wt% of 2,2-dimethoxy-2-phenylacetophenone (Ciba, Tarrytown, NY) as the photoinitiator were spread on glass microscope slides and subsequently covered by photomasks with alternating transparent or reflective bands with a periodicity of 50 μm. Monomer samples were cured under a high pressure mecury vapor arc lamp (Omnicure S-1500) equipped with a homogenizing light pipe and collimating adapter. Radiation dosage was varied by altering UV exposure time to attain specific microfeature depths as previously described [12,14]. Micropatterns substrates consisted of parallel ridges and grooves with 1–3 μm amplitudes and 50 μm periodicities for neurite contact guidance studies. Channel amplitudes and periodicities were characterized by white light interferometry using a Wyko NT 1100 optical profiling system (Veeco, Plainview, NY).

Spiral ganglion dissociated cultures

The micropatterned substrates were sterilized by 70% ethanol and UV light, then coated with poly-L-ornithine solution (Sigma-Aldrich) for 1 hour at room temperature and laminin (20 μg/ml, Sigma-Aldrich), an extracellular matrix protein, for 2 hours at 37°C. Spiral ganglion dissociated cultures were prepared as previously described [32,33]. NIH guidelines for the care and use of laboratory animals (NIH Publication #85-23 Rev. 1985) have been observed. Briefly, spiral ganglia from P3-5 rat pups were enzymatically dissociated in Ca^{2+}/Mg^{2+}-free HBSS with 0.1% collagenase (Sigma-Aldrich) and 0.125% trypsin-EDTA (Thermo Fisher Scientific, Waltham, MA), followed by mechanical dissociation using gentle blowing with pipettes. The cell suspension was plated in glass cylinders mounted on polymer substrates by sterile silicone glues. Cultures were maintained in Dulbecco's modified Eagle Medium (DMEM, Life Technologies) supplemented with N2 supplement (Life Technologies), 5% fetal bovine serum (Thermo Fisher Scientific), 10 μg/ml insulin (Sigma-Aldrich), 50 ng/ml Neurotrophin-3 (NT-3, R&D Systems, Minneapolis, MN) and 50 ng/ml Brain Derived Neurotrophic Factor (BDNF, R&D Systems) at 37°C in a 6.5% CO_2 incubator. The cultures were maintained for total of 72 hours and then fixed with 4% paraformaldehyde for 20 minutes at room temperature.

Manipulation of calcium influx and release from internal stores

Four to six hours after plating, experimental manipulations were carried out by changing culture medium. Calcium influx was increased by depolarizing with elevated extracellular K^+ - 25 mM (25K) or 50 mM (50K) - as previously described [33,34]. To decrease calcium influx, calcium-free culture media was used, in which DMEM was substituted with calcium-free DMEM (Life Technologies) with 1mM EDTA. Cadmium (Sigma-Aldrich), a non-selective voltage-gated calcium channel blocker, was added into the medium to a final concentration of 10 μM. Nifedipine (Sigma-Aldrich), an L-type Ca^{2+} channel blocker, was added to a final concentration of 1 μM. To disturb calcium release from internal stores, application of 100 μM Ryanodine (Sigma-Aldrich) or 2 μM Xestospongin C (Sigma-Aldrich) was used to block ryanodine-sensitive channels or inhibit inositol-1,4,5-trisphosphate (IP3) receptors, respectively.

Cyclic nuecleotides

To investigate the role of cyclic nucleotides in neurite guidance by micropttерned features, we used cpt-cAMP (1 mM, Sigma-Aldrich), a membrane-permeable cAMP analog, to increase cAMP activity or 8-Br-cGMP, a cell-permeable cGMP analog (20, 200 μM, Sigma-Aldrich), to increase cGMP activity.

Immunostaining

Immunolabeling of SGNs and spiral ganglion Schwann cells (SGSCs) was performed as previously described [12,35]. Anti-neurofilament 200 antibody (NF200, 1:400, Sigma-Aldrich), which labels heavy neurofilaments expressed in SGN somata and peripheral processes, and anti-S100 antibody (1:400, Sigma-Aldrich), which labels a calcium-binding protein in SGSCs, were used to identify SGNs and SGSCs, respectively. Primary antibody labeling was detected by Alexa Fluor-488 or Alexa Fluor-546 (1:800, Thermo Fisher Scientific) conjugated secondary antibodies. Nuclei were labeled with 4′,6-diamidino-2-phenylindole (DAPI) in the mounting media.

Determination of SGN survival

SGN survival was determined as previously described by scoring the total of neurons in each condition and expressed as percent of control[32,36]. Criteria for neuronal viability were NF200 immunoreactivity and a nucleus that was visible and not pyknotic.

Assessment of neurite and cell alignment

SGN neurite and SGSC alignment was measured as described previously [12,16,21]. The entire area of each culture was imaged with the micropatterns positioned parallel to horizontal and digitally stitched as one image by the “scan slide” function of Metamorph software (Molecular Devices, Silicon Valley, CA). Total neurite length (T_L) and aligned length (A_L), or the end-to-end distance of the neurite only in the direction of the micropattern features, were measured with ImageJ as previously described. The alignment ratio of T_L/A_L was used to assess the extent of neurite alignment to micropatterns. Neurites that align to and track micropattern features along their entire length result in alignment ratios close to one, while neurites that do not strongly align to the pattern yield significantly higher ratios. SGSC

alignment was measured as the angle (θ) between the micropattern direction and the major axis of an ellipse drawn around the cell body using ImageJ software (National Institutes of Health, Bethesda, MD). Angles approaching zero degrees indicate significant SGSC alignment to the micropattern.

3. Results

Intracellular calcium levels modulate neurite alignment to micropatterned features

To fabricate micropatterned substrates for neurite contact guidance studies, HMA/HDDMA formulations containing photoinitiator were exposed to UV radiation through a photomask. Photomasks used in this work have alternating parallel transparent (glass) and reflective (chrome) bands each 25 μm wide (Fig. 1A). Spatially controlling the polymerization in this manner enables micropattern formation with simple tuning of the reaction parameters facilitating modulation of micropattern features during their development (Fig. 1) [12,14]. Side view (Fig. 1B) and top-down view (Fig. 1C) scanning electron microscopic images confirm the consistency, periodicity, and amplitude of the micropatterns thus generated and used in these studies.

On unpatterned surfaces, which were exposed to UV through a blank glass slide, SGN neurites grow in random trajectories (Fig. 2A) as evidenced by a high alignment ratio, as previously described [12,14]. SGNs plated on micropatterned methacrylate substrates develop neurites that turn and align to the parallel ridge-groove line space grating (Fig. 2B) yielding an alignment ratio close to one.

To examine the influence of intracellular Ca^{2+} ($[Ca^{2+}]_i$) on SGN neurite alignment to micropatterned features, dissociated SG cultures were plated on 3 μm amplitude, 50 μm periodicity micropatterns while maintaining the culture in media with 5.4 mM K^+ or elevated K^+ (25 mM, 25 K or 50 mM, 50K). Elevation of extracellular potassium (K^+) depolarizes SGNs leading to chronic elevation of $[Ca^{2+}]_i$ via influx from voltage sensitive Ca^{2+} channels [33,34]. Treatment of SGN cultures with 25K or 50K significantly reduced neurite alignment compared to control cultures maintained in normal non-depolarizing media (Fig. 2C, D). Further, 50K disrupted alignment to a greater extent than 25K demonstrating a dose-response effect of elevated extracellular K^+. These results demonstrate that membrane depolarization, which results in elevation of $[Ca^{2+}]_i$ due to entry through voltage sensitive Ca^{2+} channels, reduces SGN alignment to microtopographical features.

Interestingly, SGN neurite alignment in cultures maintained in Ca^{2+}-free medium was similar to the alignment of neurites in medium with normal Ca^{2+} levels (Fig. 3E). Further bath application of the non-selective voltage-gated calcium channel blocker cadmium (10 μM) or L-type Ca^{2+} channel blocker nifedipine (1 μm) did not signficantly alter SGN neurite alignment (Fig. 3). Taken together, these results indicate that while entry of extracellular Ca^{2+} disrupts SGN neurite pathfinding in response to biophysical cues, it is not necessarily required within the growth cones extracellular environment to effect guidance to biophysical features.

By contrast, bath application of 100 μM Ryanodine or 2 μM Xestospongin C, which block release of internal Ca^{2+} stores via ryanodine-sensitive channels or inositol-1,4,5-trisphosphate (IP3) receptors respectively, both significantly decrease neurite alignment (Fig. 4). Thus release of Ca^{2+} from internal stores appears necessary for SGN neurite guidance by microtopographical cues.

On unpatterned tissue culture plastic coated with laminin, elevation of $[Ca^{2+}]_i$ due to membrane depolarization exerts a biphasic response on SGN survival and decreases SGN neurite growth in a dose dependent manner [33,34]. Thus, we determined SGN survival and neurite length for the various conditions used in these experiments. Table I reports these results. Consistent with prior results, elevation of extracellular K^+ to 50 mm significantly reduced SGN survival and overall neurite length [33,34]. However, neurite alignment did not appear to systematically vary with SGN survival or overall neurite length in the various treatment conditions.

Ryanodine and Xestospongin C disrupt SGSC alignment to micropatterns

SGSCs support SGN neurite growth and SC topographic features have been used to enhance directed regeneration of dorsal root ganglia axons[35,37,38]. Further, SGSCs strongly align to micropatterns, an effect that can be disrupted by inhibition of RhoA/ROCK signaling similar to the ability of RhoA and ROCK inhibitors to disrupt neurite alignment. These observations raise the possibility that SGSCs may rely on similar intracellular second messenger systems as SGNs to respond to topographical cues. To further explore this possibility, we treated SGSC cultures plated on micropatterned substrates with 3 μm amplitude and 50 μm periodicity features with ryanodine (100 μM) or Xestospongin C (2 μM). SGSC aligment was measured as the angle (θ) between the micropattern direction and the major axis of an ellipse drawn around the cell body. Angles close to zero degrees represent close alignment to the micropattern while random alignment would be yield angles near 45°. As with SGN neurites, treatment with ryanodine or Xestospongin C each significantly reduced SGSC alignment to the micropatterns (Fig. 5), suggesting that release of Ca^{2+} from internal stores is necessary for SGSC orientation to microtopographical cues.

cAMP and cGMP levels modulate SGN neurite and SGSC guidance to topographical cues

Cyclic nucleotides, including cAMP and cGMP, modulate growth cone responses to chemotactic stimuli [27,2829–31]. To determine if they similarly contribute to SGN neurite pathfinding in response to topographical features, SGN cultures plated on micropatterned substrates were treated with the cell permeant cAMP analog, cpt-cAMP or the cGMP analog, 8-Br-cGMP. Treatment of SGN cultures with cpt-cAMP (1 mM) significantly reduces SGN neurite alignment on patterned substrates with the specified amplitude and periodicity (Fig. 6).

As cAMP and cGMP often exert opposing effects on neurite guidance in response to chemotactic stimuli, we asked if elevation of cGMP could enhance SGN neurite alignment to topographical features. To uncover an enhancing effect of cGMP on neurite alignment, it is necessary to plate the cultures on micropatterns that do not exert a strong influence alignment that would obscure an enhancing effect. SGN alignment was previously shown to

correlate with pattern depth and spacing such that shallow or widely spaced features are less effective at inducing neurite alignment compared to deep or frequent features[12,14]. Accordingly, SGN cultures were maintained on substrates with shallow amplitude (e.g. 1 μm) features and wide pattern spacing so that the pattern did not exert as strong of influence on neurite growth compared to the micropatterns with 3 μm amplitudes. The alignment ratio in control cultures on these relatively shallow features with 1 μm amplitude is 1.43±0.05 (mean±SEM) in contrast to neurites that strongly align to similar patterns with a 3 μm amplitude yielding an alignment ratio of 1.11±0.01 (mean±SEM) (Figs. 2–4). Interestingly, treatment of SGN cultures with 8-Br-cGMP (20 μM) significantly increases neurite alignment on substrates with the described shallow feature pattern (Fig. 7), implying that elevation of cGMP enhances growth cone responses to topographical features. Thus, cAMP and cGMP levels appear to exert opposing influences on growth cone response to topographical cues.

Similar to the effect on SGN neurites, cpt-cAMP significantly decreases SGSC alignment to micropatterns with 3 μm amplitude features (Fig. 8), increasing the mean alignment angle from 27.4±2.0 (mean±SEM) to 41.4±2.9 on micropatterned surfaces. Meanwhile, treatment of SGSC cultures plated on with 8-Br-cGMP significantly decreases the mean alignment angle (i.e. improves alignment) on micropatterns with 1 μm amplitude (Fig. 8). Thus, elevation of cAMP levels reduces the responsiveness of both SGN neurites and SGSCs to micropatterned surfaces while elevation of cGMP levels enhances the responsiveness of SGN neurites and SGSCs to these biophysical cues.

4. Discussion

Neural prostheses suffer from poor spatial resolution compared to native neural circuits due, at least in part, to the physical distances separating the stimulating electrodes from the target neurons that they stimulate. For example, in normal cochleae, afferent SGN fibers are in intimate synaptic contact (~10 nm) with the inner hair cells. However, cochlear implant electrodes are located in the scala tympani 250–>1000 μm away from the SGNs that they activate [39]. This gap results in current spread and poor spatial signal resolution between adjacent electrodes. Thus, cochlear implant recipients typically experience poor hearing in noise and music appreciation due, in part, to non-specific neural stimulation [40,41]. Other neural prostheses (e.g. retinal implant) likewise suffer from non-specific neural stimulation and poor spatial resolution [42].

To improve the interface between neural prostheses and their target neurons, neural engineers have sought to develop biomaterials with micropatterned biochemical or, more recently, topographical surface features capable of directing neurite growth into close proximity or even contact with the electrodes [19]. For example, efforts have been made to guide SGN neurite growth towards the cochlear implant electrode arrays by topographical cues and chemotactic molecules [14–16,43–45]. Understanding the cellular processes that mediate topographical neurite guidance will enhance the ability of neural engineers to precisely guide neurite growth. Our data demonstrate that intracellular calcium and cyclic nucleotide second messenger systems participate in growth cone pathfinding in response to biophysical cues found in the developing neural microenvironment.

Many *in vitro* and *in vivo* studies demonstrate that cells in general, and neurons and their processes in particular, respond to biophysical features in their microenvironment [19], yet little is known about how cells sense topography and then respond to it. Understanding the cellular signaling events that underlie such responses will facilitate the design of surface features aimed at enhancing the integration of biomaterials with native tissue and influencing the response of the target cells to these surface features. For example, it may be possible to use small molecule inhibitors or activators of second messenger systems, such as cyclic nucleotides, to enhance the effects of topographical features to precisely guide axon regeneration.

Here we used the spatial and temporal control of photopolymerization to fabricate methacrylate platforms with precise micropatterns to probe biochemical effects on physical signaling and, ultimately, alignment of SGN neurite growth and SGSC orientation. As previously demonstrated, this photopolymerization process produces micropatterns with gradual sloping transitions between ridges and grooves. These gradual transitions facilitate studies aimed at identifying signaling events involved in topographical neurite guidance as they do not physically constrain neurites. By contrast, patterns prepared by photolithography have sharp transitions that can constrain the growth cone [46]. Without such physical constraints, the neurite response can change following manipulation of intracellular signaling events. For example, micropatterns produced by photopolymerization similar to those used in these studies facilitated the identification of transient receptor potential (TRP) cation channel subfamily V member 1 (TRPV1) and RhoA/Rho associated kinase signaling as key mediators of neurite alignment to micropatterns [21].

Calcium as a mediator of topographical guidance

Calcium is a ubiquitous second messenger that has been shown to be a critical mediator of growth cone responses to chemotactic guidance molecules. Ca^{2+} concentrations in growth cones are regulated by influx of extracellular Ca^{2+} through specific channels and by Ca^{2+} release from Ca^{2+} stores in the endoplasmic reticulum [25]. Ca^{2+} channels on the plasma membrane, such as TRP channels, voltage-dependent Ca^{2+} channels (VDCCs), and cyclic nucleotide-gated ion channels (CNGCs), mediate "Ca^{2+} influx" from the extracellular space, whereas Ca^{2+} channels on the endoplasmic reticulum (ER) membrane, such as RyRs and IP3 receptors (IP3Rs), mediate "Ca^{2+} release" from the ER Ca^{2+} stores [47]. Ca^{2+} signals from these different resources mediate growth cone steering induced by various chemotactic factors. For example, TRP channels, L-type VDCCs, and RyRs are involved in netrin-1-induced attraction [48,49]; IP3Rs are involved in NGF- and BDNF-induced attraction [50,51]; and CNGCs are involved in Sema3A-induced repulsion [52].

Further, the Ca^{2+} level in the growth cone can alter attractive and repulsive reponses of growth cones to guidance cues [26]. In some cases, Ca^{2+} release through RyRs or IP3Rs generates a steep Ca^{2+} elevation and initiates growth cone attraction [48,50,53] while Ca^{2+} influx through plasma membrane channels without Ca^{2+} release from internal Ca^{2+} stores generates a shallow Ca^{2+} elevation and initiates growth cone repulsion [24,54]. In other cases, a modest local Ca^{2+} elevation induces growth cone attraction, whereas a small local Ca^{2+} elevation (or shallow gradient across the growth cone) and large local Ca^{2+} transients induce

growth cone repulsion [24,55–57]. Thus, there is compelling evidence that chemotactic guidance cues modulate calcium dynamics in the growth cone and that, in turn, Ca^{2+} levels modulate growth cone responses to chemotactic molecules.

In a previous report, rat hippocampal neurites were shown to grow perpendicular to shallow, narrow grooves (e.g. 130 nm deep, 1 μm wide) and parallel to similar features that are deeper and wider (e.g. 1,100 nm deep, 4 μm wide) [11]. Perpendicular contact guidance was reduced by flunarizine, a N-type voltage-dependent calcium channels (VDCC), and was abolished by nifedipine and diltiazem, specific L-type VDCC antagonists suggesting that calcium influx via VDCCs is involved in perpendicular contact guidance. Conversely, parallel orientation was not perturbed by these VDCC antagonists [20]. Apparently, perpendicular and parallel contact guidance of hippocampal neurites employ different Ca^{2+} signaling mechanisms.

In this study, we increased $[Ca^{2+}]_i$ by depolarizing dissociated SGNs with elevated extracellular K^+ - 25 mM (25K) or 50 mM (50K) - as previously described [33,34]. SGN neurite alignment in cultures depolarized with 25K and 50K is significantly poorer than alignment in cultures in nondepolarized medium. Thus elevation of $[Ca^{2+}]_i$, by chronic membrane depolarization appears to disrupt SGN alignment to these micropatterns (Fig. 9). Thus, there could be an optimum intracellular calcium level necessary for contact guidance. However, entry of extracellular calcium does not appear to be necessary for contact guidance. Bath application of the general blocker of VDCCs, cadmium, or the L-type Ca^{2+} channel blocker, nifedipine, does not disrupt SGN neurite alignment, implying that external Ca^{2+} entry through VDCCs is not required for SGN process alignment to topographical features. Similarly, SGN neurite alignment in Ca^{2+}-free medium is comparable to alignment in medium with normal $[Ca^{2+}]$. These data suggest that while elevation of $[Ca^{2+}]_i$, from external sources, disrupts SGN neurite alignment to micropatterns, entry of Ca^{2+} via VDCCs is not required for SGN neurite alignment to micropatterns consisting of parallel ridges and grooves. This independence of SGNs from VDCCs to accurately track parallel features is similar to hippocampal neurites that align to parallel surface patterns [11].

Interestingly, bath application of ryanodine (100–300 μM) or Xestospongin C (2 μM), which inhibit RyR and IP3R, respectively, both significantly decrease neurite alignment suggesting that release of Ca^{2+} from internal stores is necessary for contact guidance. Thus, based on the data from this initial study, Ca^{2+} signaling in this system appears complex and likely depends on temporal and spatial dynamics.

Elevation of cGMP enhances SGN neurite alignment to microtopographical features while elevation of cAMP disrupts aligment

Cyclic nucleotides play an important role in growth cone steering by biochemical guidance cues. For example, elevation of cAMP levels is associated with attractive turning and neurite extension, even converting repulsive turning into an attractive response [24,27–29]. Likewise, elevation of cAMP levels in SGNs, as in other neurons, overcomes the inhibition of neurite growth by central glia [35,58–60]. Meanwhile, elevation of cGMP levels is generally associated with repulsive turning and growth cone collapse [29–31,61,62]. Furthermore, previous studies

suggest a complex interactive relationship between cyclic nucleotides and calcium signaling in growth cone steering [61,62].

Here we found that elevation of cAMP disrupted SGN neurite alignment to the described photopolymerized micropatterns. We also found that increasing cGMP levels enhanced SGN neurite alignment to shallow (1 μm) micropatterns, which otherwise were not of sufficient amplitude to induce significant neurite alignment. Thus, cAMP and cGMP appear to exert opposing influences on neurite aligment to microtopographical features similar to their opposing effects on chemotactive biochemical cues [63,64].

Interestingly, SGSC alignment to the micropatterns, which, like to SGN neurite alignment, depends on RhoA/ROCK signaling [21], was likewise disrupted by ryanodine and IP3 receptor inhbitors and by treatment with a cAMP analog. Further, treatment with a cGMP analog enhanced SGSC alignment to micropatterns. These data support the notion that SGN neurites and SGSCs may engage some similar signaling mechanisms to achieve alignment to topographic features. Nevertheless, these observations remain correlative and that further experiments are required to firmly establish the signaling mechanisms recruited by both SGNs and SGSCs.

Ridges of topographical features appear to activate similar signaling cascades as chemorepulsive stimuli to repel SGN growth

Neurites prefer to grow in the grooves compared to the ridges of these micropatterned substrates [12,15]. This observation implies that either the ridge features act as a repulsive signal and/or that the groove acts as a permissive substrate. We recently demonstrated that when SGN growth cones encounter the raised surfaces of the ridges intracellular signaling events are activated similar to those activated in response to chemorepulsive stimuli [21]. For example, RhoA signaling is activated while Cdc42/Rac activity is suppressed [21]. Further inhibition of TRPV1 channels reduces neurite alignment to micropatterns while induced expression of TRPV1 in 3T3 cells renders the cells sensitive to micropatterns implying that TRPV1 channels are essential for cellular guidance by physical cues. Significantly, both TRPV1 and RhoA signaling are implicated in growth cone turning in response to chemorepulsive cues. Consistent with the notion that the ridges function to repel growth cones by activating similar intracellular signaling events as chemorepulsive cues (e.g. RhoA)[21] treatment of cultures with a cAMP analog disrupts SGN neurite alignment similar to the ability of elevated cAMP levels to overcome chemorepulsive cues [35,55–57].

5. Conclusions

Here we used photopolymerization to generate specific micropatterns in methacrylate substrates that function as effective contact guidance cues to precisely direct SGN neurite growth. Such surface features could be used to guide the trajectory of regenerating SGN fibers in an effort to achieve a more intimate and precise interface with a cochlear implant electrode array. Elevation of intracellular calcium or cAMP levels significantly disrupts the alignment of SGN neurites to microtopographical patterns, while elevation of cGMP enhances alignment. The results suggest that similar intracellular signaling pathways as those recruited by chemorepulsive cues are involved in SGN neurite guidance by these

topographical features. Manipulation of these intracellular signaling pathways will be useful to further probe the strength of biophysical cues engineered for directed neural outgrowth as well as inform efforts to engineer enhanced interfaces between a neural prosthesis and its target neurons.

Acknowledgments

Supported by NIDCD (R01 DC012578, P30 DC010362), National Natural Science Foundation of China (NSFC 81171482), and the Alpha Omega Alpha Carolyn L. Kuckein Student Research Fellowship.

References

1. Joddar B, Guy AT, Kamiguchi H, Ito Y. Spatial gradients of chemotropic factors from immobilized patterns to guide axonal growth and regeneration. Biomaterials. 2013; 34(37):9593–601. [PubMed: 24021758]
2. Jang MJ, Nam Y. Geometric effect of cell adhesive polygonal micropatterns on neuritogenesis and axon guidance. J Neural Eng. 2012; 9(4):046019. [PubMed: 22814204]
3. Fricke R, Zentis PD, Rajappa LT, Hofmann B, Banzet M, Offenhausser A, Meffert SH. Axon guidance of rat cortical neurons by microcontact printed gradients. Biomaterials. 2011; 32(8):2070–6. [PubMed: 21167596]
4. Francisco H, Yellen BB, Halverson DS, Friedman G, Gallo G. Regulation of axon guidance and extension by three-dimensional constraints. Biomaterials. 2007; 28(23):3398–407. [PubMed: 17467794]
5. Gomez N, Chen S, Schmidt CE. Polarization of hippocampal neurons with competitive surface stimuli: contact guidance cues are preferred over chemical ligands. J R Soc Interface. 2007; 4(13): 223–33. [PubMed: 17251152]
6. Krsko P, McCann TE, Thach TT, Laabs TL, Geller HM, Libera MR. Length-scale mediated adhesion and directed growth of neural cells by surface-patterned poly(ethylene glycol) hydrogels. Biomaterials. 2009; 30(5):721–9. [PubMed: 19026443]
7. Lee JY, Bashur CA, Gomez N, Goldstein AS, Schmidt CE. Enhanced polarization of embryonic hippocampal neurons on micron scale electrospun fibers. J Biomed Mater Res A. 2010; 92(4):1398–406. [PubMed: 19353562]
8. Fozdar DY, Lee JY, Schmidt CE, Chen S. Selective axonal growth of embryonic hippocampal neurons according to topographic features of various sizes and shapes. Int J Nanomedicine. 2011; 6:45–57.
9. Fozdar DY, Lee JY, Schmidt CE, Chen S. Hippocampal neurons respond uniquely to topographies of various sizes and shapes. Biofabrication. 2010; 2(3):035005. [PubMed: 20823503]
10. Dowell-Mesfin NM, Abdul-Karim MA, Turner AM, Schanz S, Craighead HG, Roysam B, Turner JN, Shain W. Topographically modified surfaces affect orientation and growth of hippocampal neurons. J Neural Eng. 2004; 1(2):78–90. [PubMed: 15876626]
11. Rajnicek A, Britland S, McCaig C. Contact guidance of CNS neurites on grooved quartz: influence of groove dimensions, neuronal age and cell type. J Cell Sci. 1997; 110(Pt 23):2905–13. [PubMed: 9359873]
12. Clarke JC, Tuft BW, Clinger JD, Levine R, Figueroa LS, Guymon CA, Hansen MR. Micropatterned methacrylate polymers direct spiral ganglion neurite and Schwann cell growth. Hear Res. 2011; 278(1–2):96–105. [PubMed: 21616131]
13. Miller C, Jeftinija S, Mallapragada S. Micropatterned Schwann cell-seeded biodegradable polymer substrates significantly enhance neurite alignment and outgrowth. Tissue Eng. 2001; 7(6):705–15. [PubMed: 11749728]
14. Tuft BW, Li S, Xu L, Clarke JC, White SP, Guymon BA, Perez KX, Hansen MR, Guymon CA. Photopolymerized microfeatures for directed spiral ganglion neurite and Schwann cell growth. Biomaterials. 2013; 34(1):42–54. [PubMed: 23069708]

15. Tuft BW, Xu L, White SP, Seline AE, Erwood AM, Hansen MR, Guymon CA. Neural pathfinding on uni- and multidirectional photopolymerized micropatterns. ACS Appl Mater Interfaces. 2014; 6(14):11265–76. [PubMed: 24911660]
16. Tuft BW, Zhang L, Xu L, Hangartner A, Leigh B, Hansen MR, Guymon CA. Material stiffness effects on neurite alignment to photopolymerized micropatterns. Biomacromolecules. 2014; 15(10):3717–27. [PubMed: 25211120]
17. O'Donnell M, Chance RK, Bashaw GJ. Axon growth and guidance: receptor regulation and signal transduction. Annu Rev Neurosci. 2009; 32:383–412. [PubMed: 19400716]
18. Song H, Poo M. The cell biology of neuronal navigation. Nat Cell Biol. 2001; 3(3):E81–8. [PubMed: 11231595]
19. Hoffman-Kim D, Mitchel JA, Bellamkonda RV. Topography, cell response, and nerve regeneration. Annu Rev Biomed Eng. 2010; 12:203–31. [PubMed: 20438370]
20. Rajnicek A, McCaig C. Guidance of CNS growth cones by substratum grooves and ridges: effects of inhibitors of the cytoskeleton, calcium channels and signal transduction pathways. J Cell Sci. 1997; 110(Pt 23):2915–24. [PubMed: 9359874]
21. Li S, Tuft BW, Xu L, Polacco MA, Clarke JC, Guymon CA, Hansen MR. Microtopographical features generated by photopolymerization recruit RhoA/ROCK through TRPV1 to direct cell and neurite growth. Biomaterials. 2015; 53:95–106. [PubMed: 25890710]
22. Gomez TM, Zheng JQ. The molecular basis for calcium-dependent axon pathfinding. Nat Rev Neurosci. 2006; 7(2):115–25. [PubMed: 16429121]
23. Henley J, Poo MM. Guiding neuronal growth cones using Ca2+ signals. Trends Cell Biol. 2004; 14(6):320–30. [PubMed: 15183189]
24. Henley JR, Huang KH, Wang D, Poo MM. Calcium mediates bidirectional growth cone turning induced by myelin-associated glycoprotein. Neuron. 2004; 44(6):909–16. [PubMed: 15603734]
25. Tojima T, Hines JH, Henley JR, Kamiguchi H. Second messengers and membrane trafficking direct and organize growth cone steering. Nat Rev Neurosci. 2011; 12(4):191–203. [PubMed: 21386859]
26. Zheng JQ. Turning of nerve growth cones induced by localized increases in intracellular calcium ions. Nature. 2000; 403(6765):89–93. [PubMed: 10638759]
27. Murray AJ, Tucker SJ, Shewan DA. cAMP-dependent axon guidance is distinctly regulated by Epac and protein kinase A. J Neurosci. 2009; 29(49):15434–44. [PubMed: 20007468]
28. Lohof AM, Quillan M, Dan Y, Poo MM. Asymmetric modulation of cytosolic cAMP activity induces growth cone turning. J Neurosci. 1992; 12(4):1253–61. [PubMed: 1372932]
29. Song H, Ming G, He Z, Lehmann M, McKerracher L, Tessier-Lavigne M, Poo M. Conversion of neuronal growth cone responses from repulsion to attraction by cyclic nucleotides. Science. 1998; 281(5382):1515–8. [PubMed: 9727979]
30. Song HJ, Ming GL, Poo MM. cAMP-induced switching in turning direction of nerve growth cones. Nature. 1997; 388(6639):275–9. [PubMed: 9230436]
31. Ming GL, Song HJ, Berninger B, Holt CE, Tessier-Lavigne M, Poo MM. cAMP-dependent growth cone guidance by netrin-1. Neuron. 1997; 19(6):1225–35. [PubMed: 9427246]
32. Hansen MR, Zha XM, Bok J, Green SH. Multiple distinct signal pathways, including an autocrine neurotrophic mechanism, contribute to the survival-promoting effect of depolarization on spiral ganglion neurons in vitro. J Neurosci. 2001; 21(7):2256–67. [PubMed: 11264301]
33. Hegarty JL, Kay AR, Green SH. Trophic support of cultured spiral ganglion neurons by depolarization exceeds and is additive with that by neurotrophins or cAMP and requires elevation of [Ca2+]i within a set range. J Neurosci. 1997; 17(6):1959–70. [PubMed: 9045725]
34. Roehm PC, Xu N, Woodson EA, Green SH, Hansen MR. Membrane depolarization inhibits spiral ganglion neurite growth via activation of multiple types of voltage sensitive calcium channels and calpain. Mol Cell Neurosci. 2008; 37(2):376–87. [PubMed: 18055215]
35. Jeon EJ, Xu N, Xu L, Hansen MR. Influence of central glia on spiral ganglion neuron neurite growth. Neuroscience. 2011; 177:321–34. [PubMed: 21241783]
36. Hansen A, Rolen SH, Anderson K, Morita Y, Caprio J, Finger TE. Correlation between olfactory receptor cell type and function in the channel catfish. J Neurosci. 2003; 23(28):9328–39. [PubMed: 14561860]

37. Lopez-Fagundo C, Mitchel JA, Ramchal TD, Dingle YT, Hoffman-Kim D. Navigating neurites utilize cellular topography of Schwann cell somas and processes for optimal guidance. Acta Biomater. 2013; 9(7):7158–68. [PubMed: 23557939]
38. Whitlon DS, Tieu D, Grover M, Reilly B, Coulson MT. Spontaneous association of glial cells with regrowing neurites in mixed cultures of dissociated spiral ganglia. Neuroscience. 2009; 161(1): 227–35. [PubMed: 19324078]
39. Hassepass F, Bulla S, Maier W, Laszig R, Arndt S, Beck R, Traser L, Aschendorff A. The new mid-scala electrode array: a radiologic and histologic study in human temporal bones. Otol Neurotol. 2014; 35(8):1415–20. [PubMed: 24836594]
40. Esquia Medina GN, Borel S, Nguyen Y, Ambert-Dahan E, Ferrary E, Sterkers O, Grayeli AB. Is electrode-modiolus distance a prognostic factor for hearing performances after cochlear implant surgery? Audiol Neurootol. 2013; 18(6):406–13. [PubMed: 24157488]
41. Filipo R, Mancini P, Panebianco V, Viccaro M, Covelli E, Vergari V, Passariello R. Assessment of intracochlear electrode position and correlation with behavioural thresholds in CII and 90K cochlear implants. Acta Otolaryngol. 2008; 128(3):291–6. [PubMed: 18274915]
42. Fornos AP, Sommerhalder J, Pelizzone M. Reading with a simulated 60-channel implant. Front Neurosci. 2011; 5:57. [PubMed: 21625622]
43. Reich U, Fadeeva E, Warnecke A, Paasche G, Muller P, Chichkov B, Stover T, Lenarz T, Reuter G. Directing neuronal cell growth on implant material surfaces by microstructuring. J Biomed Mater Res B Appl Biomater. 2012; 100(4):940–7. [PubMed: 22287482]
44. Schlie-Wolter S, Deiwick A, Fadeeva E, Paasche G, Lenarz T, Chichkov BN. Topography and coating of platinum improve the electrochemical properties and neuronal guidance. ACS Appl Mater Interfaces. 2013; 5(3):1070–7. [PubMed: 23327880]
45. Tan F, Walshe P, Viani L, Al-Rubeai M. Surface biotechnology for refining cochlear implants. Trends Biotechnol. 2013; 31(12):678–87. [PubMed: 24404581]
46. Johansson F, Carlberg P, Danielsen N, Montelius L, Kanje M. Axonal outgrowth on nano-imprinted patterns. Biomaterials. 2006; 27(8):1251–8. [PubMed: 16143385]
47. Berridge MJ, Bootman MD, Roderick HL. Calcium signalling: dynamics, homeostasis and remodelling. Nat Rev Mol Cell Biol. 2003; 4(7):517–29. [PubMed: 12838335]
48. Hong K, Nishiyama M, Henley J, Tessier-Lavigne M, Poo M. Calcium signalling in the guidance of nerve growth by netrin-1. Nature. 2000; 403(6765):93–8. [PubMed: 10638760]
49. Wang GX, Poo MM. Requirement of TRPC channels in netrin-1-induced chemotropic turning of nerve growth cones. Nature. 2005; 434(7035):898–904. [PubMed: 15758951]
50. Akiyama H, Matsu-ura T, Mikoshiba K, Kamiguchi H. Control of neuronal growth cone navigation by asymmetric inositol 1,4,5-trisphosphate signals. Sci Signal. 2009; 2(79):ra34. [PubMed: 19602704]
51. Li Y, Jia YC, Cui K, Li N, Zheng ZY, Wang YZ, Yuan XB. Essential role of TRPC channels in the guidance of nerve growth cones by brain-derived neurotrophic factor. Nature. 2005; 434(7035): 894–8. [PubMed: 15758952]
52. Togashi K, von Schimmelmann MJ, Nishiyama M, Lim CS, Yoshida N, Yun B, Molday RS, Goshima Y, Hong K. Cyclic GMP-gated CNG channels function in Sema3A-induced growth cone repulsion. Neuron. 2008; 58(5):694–707. [PubMed: 18549782]
53. Jin M, Guan CB, Jiang YA, Chen G, Zhao CT, Cui K, Song YQ, Wu CP, Poo MM, Yuan XB. Ca2+-dependent regulation of rho GTPases triggers turning of nerve growth cones. J Neurosci. 2005; 25(9):2338–47. [PubMed: 15745960]
54. Ooashi N, Futatsugi A, Yoshihara F, Mikoshiba K, Kamiguchi H. Cell adhesion molecules regulate Ca2+-mediated steering of growth cones via cyclic AMP and ryanodine receptor type 3. J Cell Biol. 2005; 170(7):1159–67. [PubMed: 16172206]
55. Zheng JQ, Poo MM. Calcium signaling in neuronal motility. Annu Rev Cell Dev Biol. 2007; 23:375–404. [PubMed: 17944572]
56. Robles E, Huttenlocher A, Gomez TM. Filopodial calcium transients regulate growth cone motility and guidance through local activation of calpain. Neuron. 2003; 38(4):597–609. [PubMed: 12765611]

57. Wen Z, Guirland C, Ming GL, Zheng JQ. A CaMKII/calcineurin switch controls the direction of Ca(2+)-dependent growth cone guidance. Neuron. 2004; 43(6):835–46. [PubMed: 15363394]

58. Cai D, Qiu J, Cao Z, McAtee M, Bregman BS, Filbin MT. Neuronal cyclic AMP controls the developmental loss in ability of axons to regenerate. J Neurosci. 2001; 21(13):4731–9. [PubMed: 11425900]

59. Hannila SS, Filbin MT. The role of cyclic AMP signaling in promoting axonal regeneration after spinal cord injury. Exp Neurol. 2008; 209(2):321–32. [PubMed: 17720160]

60. Qiu J, Cai D, Dai H, McAtee M, Hoffman PN, Bregman BS, Filbin MT. Spinal axon regeneration induced by elevation of cyclic AMP. Neuron. 2002; 34(6):895–903. [PubMed: 12086638]

61. Forbes EM, Thompson AW, Yuan J, Goodhill GJ. Calcium and cAMP Levels Interact to Determine Attraction versus Repulsion in Axon Guidance. Neuron. 2012; 74(3):490–503. [PubMed: 22578501]

62. Nishiyama M, Hoshino A, Tsai L, Henley JR, Goshima Y, Tessier-Lavigne M, Poo MM, Hong K. Cyclic AMP/GMP-dependent modulation of Ca2+ channels sets the polarity of nerve growth-cone turning. Nature. 2003; 423(6943):990–5. [PubMed: 12827203]

63. Averaimo S, Nicol X. Intermingled cAMP, cGMP and calcium spatiotemporal dynamics in developing neuronal circuits. Front Cell Neurosci. 2014; 8:376. [PubMed: 25431549]

64. Piper M, van Horck F, Holt C. The role of cyclic nucleotides in axon guidance. Adv Exp Med Biol. 2007; 621:134–43. [PubMed: 18269216]

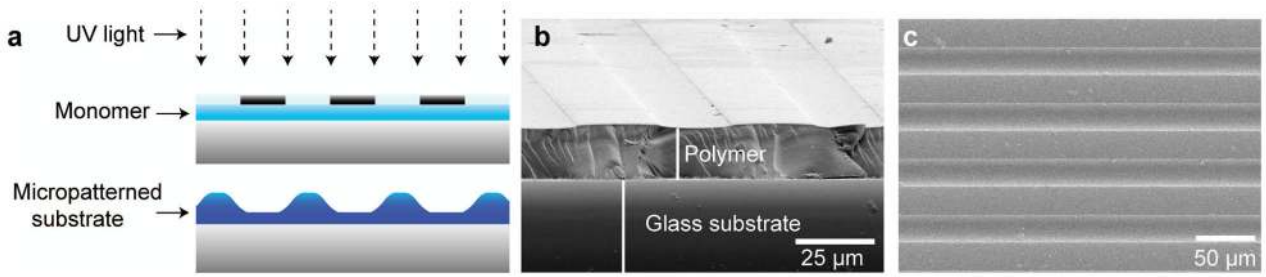

Figure 1.

Generation of micropatterned HMA-co-HDDMA polymer surfaces. **a**. Schematic of photopatterning process. A photomask allows selectively exposure of photopolymerizable monomer to UV light resulting in a pattern of raised microfeatures across the surface**. b, c.** Side view (b) and top-down view (c) of representative SEM images of micropatterned polymers with 50 μm periodicity.

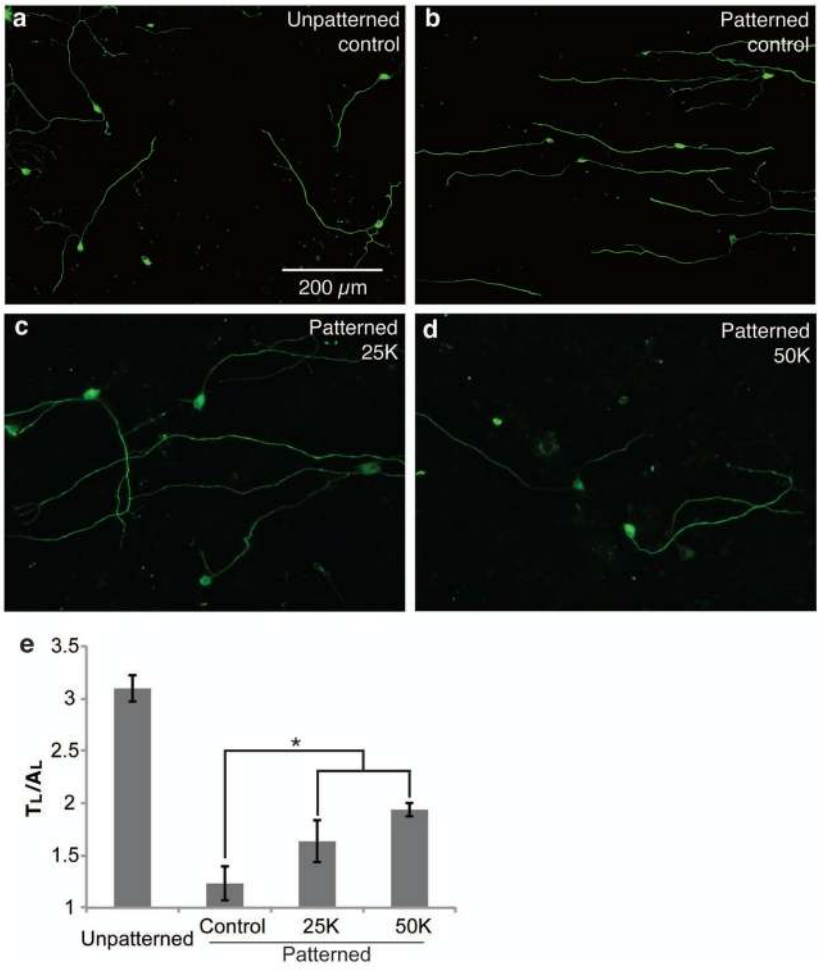

Figure 2.

Membrane depolarization reduces SG neurite alignment to micropatterns. **a, b**. Representive images of SG neurite alignment in cultures plated on unpatterned surface (a) and micropatterned surfaces (b). **c–d**. Representive images of SG neurite alignment in cultures plated on micropatterned surfaces and maintained in 25K medium (c) or 50K medium (d). **e**. Membrane depolarization with 25K (n = 191) and 50K (n=36) media decreased neurite alignment compared to control (n = 163). All micropatterns had 2 μm amplitutude and 50 μm periodicity with a horizontal direction in the figures unless specified otherwise. *p < 0.05, Kruskal-Wallis one way ANOVA on ranks followed by Dunn's method. Data represent mean ± SEM.

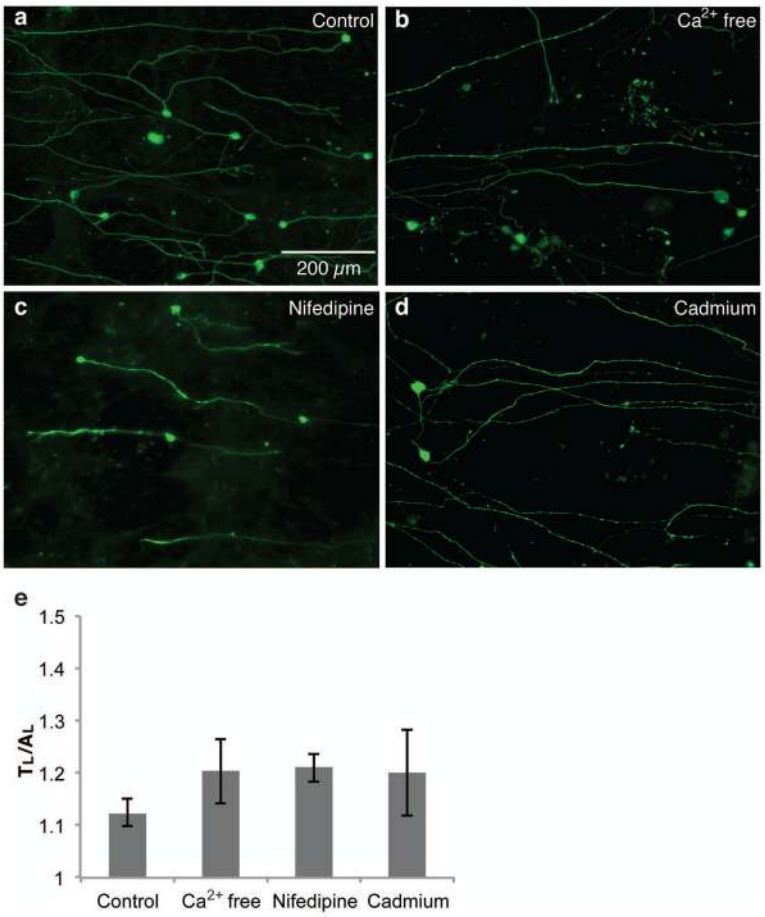

Figure 3.

Inhibition of calcium influx fails to disturb SG neurite alignment to micropatterns. **a**. Images of SG neurite alignment in cultures plated on micropatterned surfaces (a). **b–d**. Representive images of SG neurite alignment in cultures plated on micropatterned surfaces and maintained in Ca^{2+}-free medium (b), in presence of nifedipine (c) and cadmium (d). **e**. Inhibition of calcium influx by bath application of nifedipine (1μM, n = 141), cadmium (10 μM, n= 67), or calcium free medium (n = 26) did not significantly perturb neurite alignment by Kruskal-Wallis one way ANOVA on ranks. Data represent mean ± SEM.

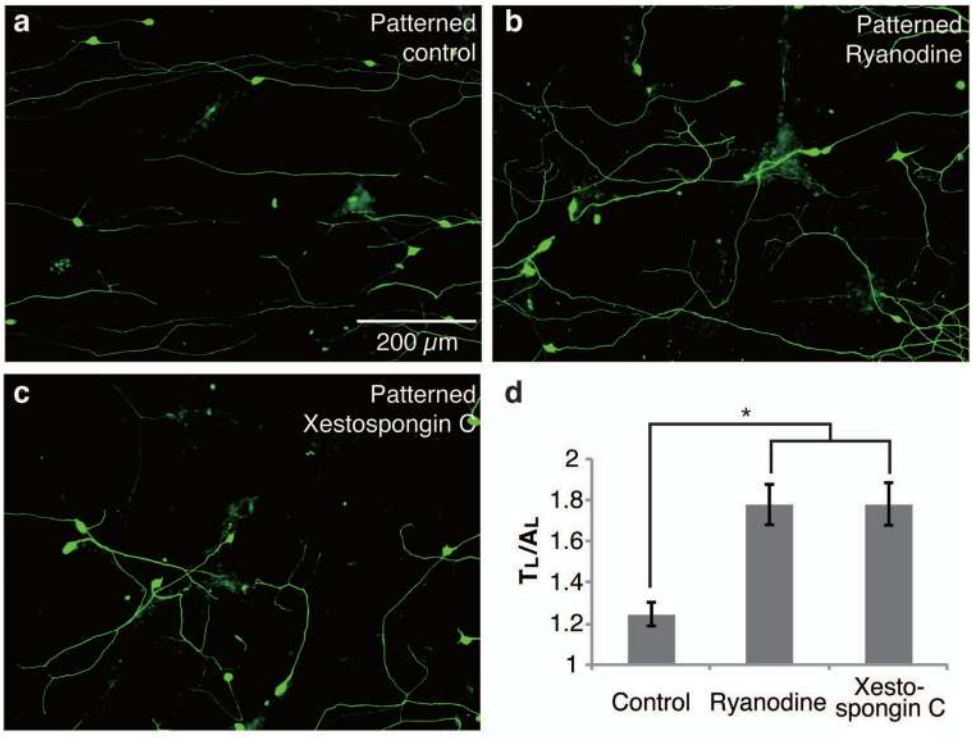

Figure 4.

Inhibition of calcium release from internal calcium store reduces SG neurite alignment to micropatterns. **a–c.** Images of SG neurite alignment in cultures plated on micropatterned surfaces in control medium (a), in the presence of ryanodine (b) or Xestospongin C (c). **d**. Bath application of ryanodine (100 μM, n = 102) or Xestospongin C (2 μM, n = 76) both significantly decreased neurite alignment compared to the control (n = 80). *$p < 0.05$, Kruskal-Wallis one way ANOVA on ranks followed by Dunn's method. Data represent mean ± SEM.

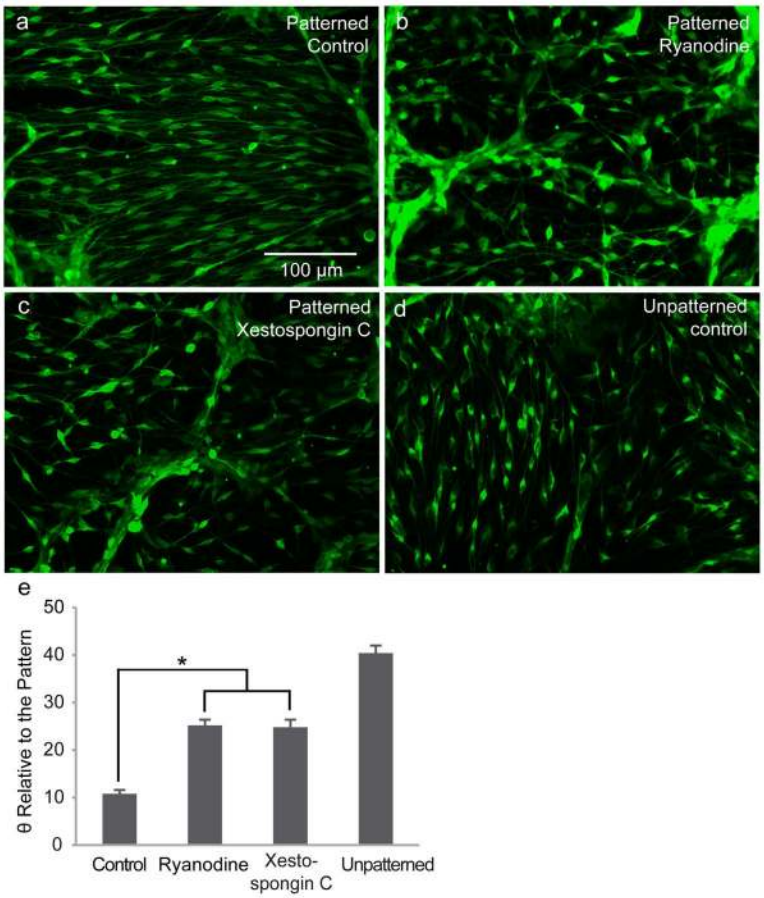

Figure 5.

Inhibition of calcium release from internal calcium store reduces SGSC alignment to micropatterns. **a–c.** Images of SGSC alignment in cultures plated on micropatterned surfaces in control medium (a), in the presence of ryanodine (b) or Xestospongin C (c). **d**. Bath application of ryanodine (100 μM, n = 102) or Xestospongin C (2 μM, n = 76) both significantly decreased neurite alignment compared to the control (n = 80). *$p < 0.05$, Kruskal-Wallis one way ANOVA on ranks followed by Dunn's method. Data represent mean ± SEM.

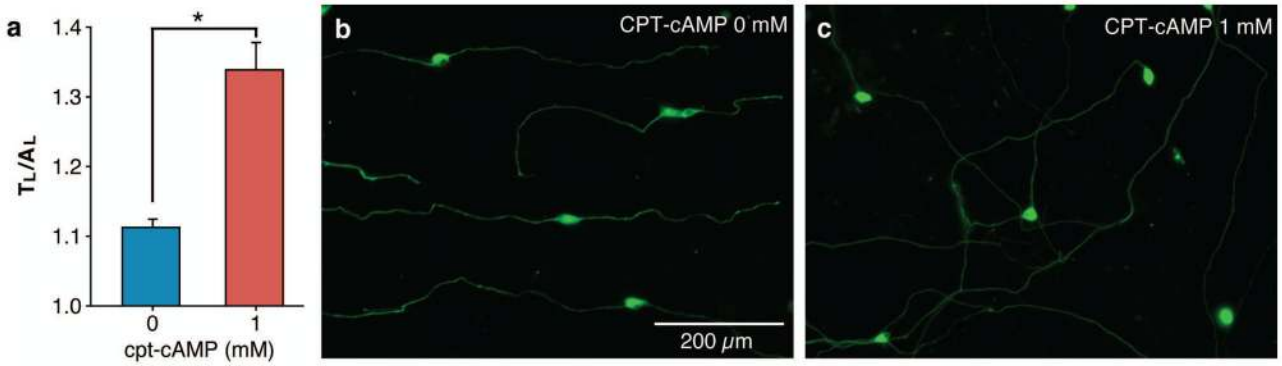

Figure 6.

Elevation of cAMP levels disrupts SGN neurite alignment to micropatterns. **a**. Treatment of SGNs with cpt-cAMP (1 mM, $n = 200$), a cell permeant cAMP analog, significantly reduces SGN neurite alignment to micropatterns compared to SGN neurites maintained in the absence of cpt-cAMP ($n = 100$). **b–c.** Images of SGN neurite alignment in cultures plated on micropatterned surfaces and maintained in the absence (b) or presence (c) of cpt-cAMP. *$p < 0.05$, Mann-Whitney test. Data represent mean ± SEM.

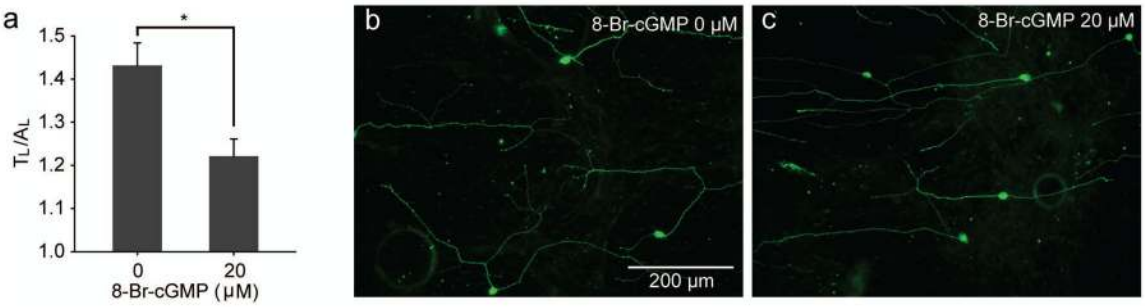

Figure 7.

Elevation of cGMP levels enhances SGN neurite alignment to micropatterns. **a**. Treatment of SGNs with 8-Br-cGMP (cGMP, 20 μM, $n = 119$; 200 μM, $n = 136$) significantly increases SGN neurite alignment to micropatterns compared to SGN neurites maintained in the absence of cGMP ($n = 236$). **b–d**. Images of SGN neurite alignment in cultures plated on micropatterned surfaces and maintained in the absence (b) or presence (c–d) of cGMP. *$p < 0.05$, Mann-Whitney test. Data represent means ± SEM. Data represent means ± SEM. All micropatterns had 1 μm amplitutude and 50 μm periodicity with a horizontal direction.

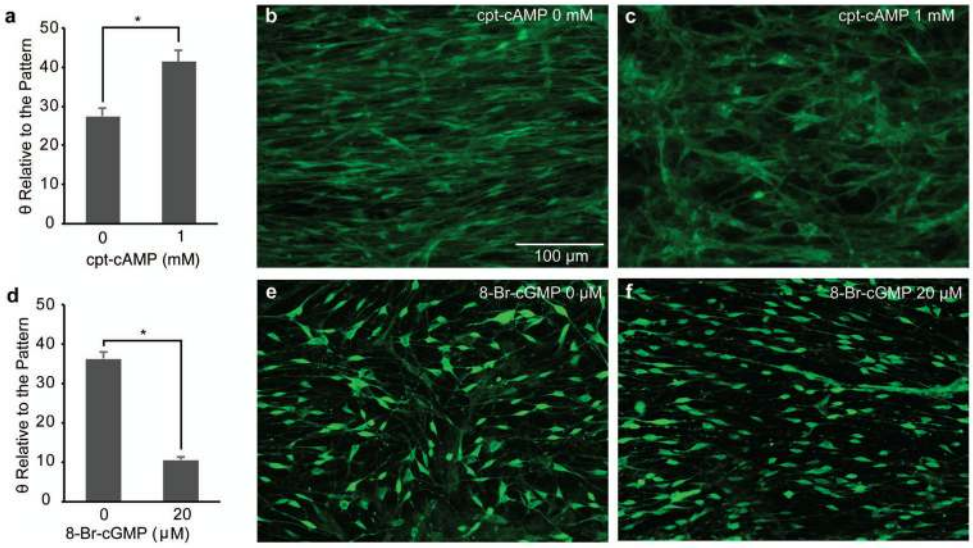

Figure 8.

Elevation of cAMP levels disrupts SGSCs alignment to micropatterns while elevation of cGMP levels enhances alignment. **a**. Treatment of SGSC cultures with cpt-cAMP (1 mM, n = 197) significantly reduces SGSC alignment to micropatterns compared to SGSCs maintained in the absence of cpt-cAMP (n = 188). **b–c**. Images of SGSC alignment in cultures plated on micropatterned surfaces and maintained in the absence (**b**) or presence (**c**) of cpt-cAMP. *p < 0.05, Mann-Whitney test. Data represent means ± SEM.

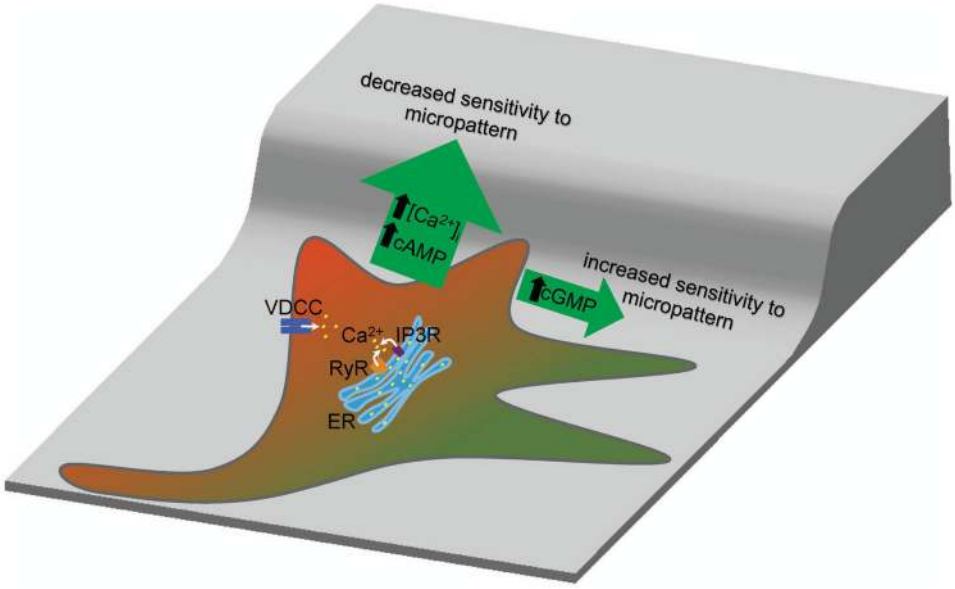

Figure 9.

Schematic of the effects of Ca^{2+} and cyclic nucleotide second messengers systems on growth cone sensitivity to micropatterns. Ridges of micropatterns function to repel neurite growth (red shade) and induce neurite extension within grooves (green shade). Membrane depolarization with elevated K^+ increases $[Ca^{2+}]_i$ via entry through voltage dependent Ca^{2+} channels (VDCC) and decreases SGN sensitivity to micropatterns manifest as neurite extension across the ridges. However, entry of extracellular Ca^{2+} is not required for the growth cone to respond to the micropattern. Meanwhile, inhibition of Ca^{2+} release from internal stores (e.g. in the endoplasmic reticulum, ER) by blocking ryanodine receptors (RyR) or inositol triphosphate receptors (IP3R) also reduces sensitivity to the micropattern. The cyclic nucleotides, cAMP and cGMP, function in opposition with each other. Elevation of cAMP reduces sensitivity while elevation of cGMP increases sensitivity to the micropattern.

Table I

SGN survival and neurite length.

	Mean survival (percent control)	SEM	p value <0.05	Mean neurite length (μm)	SEM	p value <0.05
Control	100.00%	10.18%		422.25	15.46	
25K	83.18%	7.32%	N	382.73	9.79	N
50K	42.84%	4.45%	Y	294.24	22.11	Y
Ca^{2+} free	98.20%	11.06%	N	358.14	36.72	N
Nifedipine	109.79%	15.44%	N	417.22	14.30	N
Cadmium	114.62%	14.65%	N	449.63	20.23	N
Ryanodine	108.59%	10.18%	N	407.28	14.48	N
Xestospongin C	109.57%	12.61%	N	362.60	14.44	N
cpt-cAMP	97.60%	3.68%	N	568.55	36.34	Y
8-Br-cGMP	82.52%	20.85%	N	488.00	17.09	Y

Statistical significance compared to control by one-way ANOVA on ranks followed by Dunn's post-hoc test. SEM=standard error of mean.